Fibroblast activation protein enzyme deficiency prevents liver steatosis, insulin resistance and glucose intolerance and increases fibroblast growth factor-21 in diet induced obese mice

Sumaiya Chowdhury, Sunmi Song, Hui Emma Zhang, Xin Maggie Wang, Margaret G. Gall, Denise Ming Tse Yu, Angelina J. Lay, Michelle Sui Wen Xiang, Kathryn A. Evans, Stefanie Wetzel, Yolanda Liu, Belinda Yau, Andrew L. Coppage, Lisa Lo, Rebecca A. Stokes, Wayne J. Hawthorne, Gregory J. Cooney, Susan V. McLennan, Jenny E. Gunton, William W. Bachovchin, Nigel Turner, Melkam A. Kebede, Geoffrey W. McCaughan, Stephen M. Twigg, Mark D. Gorrell

Supplementary Material:

Supplementary Method:

Generation of the FAP gene knock-in (gki) mouse strain

Fap conditional and constitutive knock-in mice containing the point mutation Ser624Ala, which ablates catalytic activity, [1] were generated by Ozgene (Bentley, Western Australia) using standard techniques. A “floxed” “mini cDNA cassette, cloned into intron 21 approximately 100 bp upstream of exon 22 (E22) (Fig. S1), consisted of a fused exon (E22-E26) derived from wildtype *Fap* cDNA (OriGene, Rockville, MD; #BC019190) followed by a polyadenylation signal (pA) to terminate transcription and thus force expression of wildtype *Fap*; and further followed by a *PGK-neomycin* selection cassette flanked by *FRT* sites. The TCC to GCC point mutation (Ser624Ala) was targeted into the first codon of endogenous E22 downstream of the mini cDNA cassette and the selection cassette.

$Fap^{wt/flox}$ neomycin-resistant C57BL/6 Bruce4 embryonic stem (ES) cell clones were identified by Southern blot analyses (Fig. S2) and microinjected into BALB/c blastocysts for generation of $Fap^{wt/flox}$ mice. $Fap^{wt/conKI}$ mice, which express the wildtype *Fap* mini cDNA cassette, were generated by *flp*-mediated excision of the *PGK-neomycin* selection cassette. $Fap^{wt/KI}$ (heterozygote FAPgki) mice were generated by *cre*-mediated excision of the wildtype *Fap* mini cDNA cassette. All ES clones and mice were screened and verified by Southern Blot analyses (Fig. S2). Putative FAPgki mice were also screened by specific FAP enzyme assay of plasma [2] (Fig. S3A). We previously showed that human FAPSer624Ala is cell surface expressed and bound by the F19 MAb, which depends upon

correct protein conformation [1, 3]. As evidence for correct protein folding of FAP in mice that carry this mutation, we showed that cell surface expression of FAP was not diminished by Ser624Ala point mutation in the FAPgki mice (Fig. S3B).

Supplementary Method:

Cell surface expression of FAP on fibroblasts

Lung was harvested from FAPgki mouse and cut into ~1 mm pieces that were digested with 0.5 mg/ml collagenase at 37°C for 30 min, then pushed through a 70 µm cell strainer. After centrifugation at 1200 rpm for 5 min, cells were resuspended in complete media (DMEM with 10% FCS, antibiotic and Amphotericin B) and cultured. For flow cytometry, confluent fibroblasts were harvested as cell suspensions using trypleE (Cat. no. 12605, Thermo Scientific, Carlsbad, CA, USA). Briefly, cells were fixed in 2% (v/v) paraformaldehyde (Cat. no. 18814, Polysciences, Warrington, PA, USA) and stained with primary antibody against FAP (Cat. no. BAF3715, R&D Systems, Minneapolis, MN, USA) or normal sheep IgG (Cat. no. 31243, Thermo Fisher Scientific) as a negative control. Cells were analyzed on Cano II (BD Biosciences). Flow cytometric data were analyzed with FlowJo software version 9.9 (TreeStar, Ashland, Ore).

Supplementary Method:

Plasma GLP-1

For GLP-1 assay, blood samples were collected from fasting mice and mice after 15 min post glucose challenge. Glucose (2 g/kg body weight) was administered by oral gavage following 6 h fasting. Blood samples were collected on ice in 1 mL EDTA tubes (Mini Collect®, Kremsmunster, Austria). Prior to blood collection, DPP4 inhibitor, Sitagliptin (Merck, NJ, USA) was added to the tubes for a final concentration of 10 uM, to prevent ex vivo degradation of GLP-1 in the blood. Blood was centrifuged at 3000 g for 5 min and supernatant (plasma) was stored at -80°C. All steps were performed at 4°C. Active GLP-1 was measured using GLP-1 ELISA kit (Cat. No. #81508) (Crystal Chem, IL, USA) according to manufacturers instructions.

Supplementary Method:

Diets:

Mice were given ad libitum access to water and either chow diet (8% kcal fat, 21% kcal protein, 71% kcal carbohydrate; Gordon's Specialty Stock Feeds, Yanderra, NSW, Australia or Specialty Feeds, WA, Australia) (control group) or to High Fat Diet (HFD).

Each HFD cage had non-edible alpha-dri bedding and, for dental health, a wooden chew block (cat no. ASAEC-A, Able Scientific, WA, Australia). HFD was purchased (Specialty Feeds; Cat. No. SF03-020) or made in-house. The Specialty Feeds HFD was hydrogenated vegetable oil (Copha) based and contained 43% kcal fat, 17% kcal protein, 40% kcal carbohydrate (with 0.19% weight/volume cholesterol) as it is designed to be atherogenic and diabetogenic (Specialty Feeds catalogue, 2009). The in-house HFD was based on rodent diet D12451 of Research Diets (New Brunswick, NJ, USA) [4, 5]. The detail of this lard based in-house HFD, which contains 45% kcal fat, 20% kcal protein, 35% kcal carbohydrate, is published [4]. Weight gain by WT mice was similar between chow and γ-irradiated HFD, so when γ-irradiation of commercially supplied HFD became mandatory in our animal facility, only in-house HFD was used.

Supplementary Method:

Immunohistochemistry and immunofluorescence stain

Liver paraffin sections at 5 μm were rehydrated and then antigen retrieved using proteinase K (20 μg/ml) for 20 min. F4/80 antibody supernatant (Gift from Dr S Tikoo) at 10 μg/ml was incubated for 1.5 hour at room temperature, with rat IgG as a control. After repeated washes in PBS, sections were incubated for 30 min with horseradish peroxidase (HRP)-conjugated secondary antibody (Dako, Glostrup, Denmark). The chromogenic reaction employed 3,3-diaminobenzidine (DAB) with H_2O_2. Liver frozen sections at 5 μm were fixed with 4% PFA and blocked with BSA. Primary antibody to CD36 (AF2519, R&D) at 33 ng/ml was incubated for 1.5 h at room temperature followed by a AF488-labelled donkey anti-sheep antibody then DAPI to counterstain nuclei. Quantification of immunostains used an LAS image software package, version 4.8. Total F4/80 staining was expressed as percentage of F4/80 immunostain in the assessed liver area at 10x magnification. Fluorescence intensity of CD36 immunostaining from four fields per section at 200x magnification was quantified in arbitrary units of fluorescent signal at 488 nm absorbance.

Table S1. The genes studied by Taqman gene expression assay.

Gene Name	Gene ID	Assay ID
Acetyl-Coenzyme A carboxylase alpha	*Acc*	Mm01304276_m1
Apolipoprotein C3	*Apoc3*	Mm00445670_m1
Carnitine palmitoyltransferase 1	*Cpt1*	Mm00550438_m1
CD36 Antigen	*Cd36*	Mm01135198_m1
Carbohydrate Response Element Binding Protein; MLX Interacting Protein Like	*Chrebp; Mlxipl*	Mm00498811_m1
Dipeptidyl peptidase 4	*Dpp4*	Mm00494548_m1
Dipeptidyl peptidase 8	*Dpp8*	Mm00547049_m1
Dipeptiyl peptidase 9	*Dpp9*	Mm00841122_m1
Eukaryotic 18S rRNA	*18S*	Hs99999901_s1
Fatty acid synthase	*Fasn*	Mm00662319_m1
Fibroblast activation protein	*Fap*	Mm00484254_m1
Fibroblast growth factor 21	*Fgf21*	Mm00840165_g1
Glucokinase	*Gck*	Mm00439129_m1
Low density lipoprotein receptor	*Ldlr*	Mm01177349_m1
Lipin1	*Lipin-1*	Mm00550511_m1
Peroxisome proliferative activated receptor gamma	*Ppar-γ*	Mm01184322_m1
Peroxisome proliferator activated receptors α	*Pparα*	Mm00627559_m1
Sterol regulatory element binding protein-1c	*Srebp1-c*	Mm00550338_m1
Eukaryotic 18S rRNA*	18S	Hs99999901_s1
Beta-actin*	*Actb*	Mm00607939_s1

- Housekeeping gene.

Table S2. All data of human pancreas samples obtained from nPOD.

FAP Activity (Δpmol AMC/min/mg Protein)	Donor Type	AutoAb (RIA)	Age (years)	Diabetes Duration (years)	Gender	Ethnicity	C-peptide (ng/ml)	HbA1c	BMI	Clinical History	Cause of Death	Histopathology	Comment
3.943	No diabetes	Negative	59		Female	Caucasian	9.89		24.8			Ins+/Gluc+ normal islets. Fatty infiltration-mild	
5.664	No diabetes	Negative	30		Male	Caucasian	17.91		20.6			Ins+/Gluc+ normal islets. Insulin+ less intense and distinct as for most ot...	
22.957	No diabetes	Negative	27		Male	Hispanic	9.09		19.1			Normal. Very mild, acute pancreatitis.	Very faint glucagon. Repeating stains.
4.044	No diabetes	Negative	27.1		Male	Caucasian	7.71	6.3	35.6			Ins+/Gluc+ normal islets, many large especially in head and body. Degree of...	Multifocal, mild ductular mucinous metaplasia.
5.432	No diabetes	Negative	45.1		Female	Caucasian	0.55	6.1	35.1	Hypertension Father had diabetes and stroke.		Ins+/Gluc+ islets. Multifocal, mild periductal and peri-islet fibrosis. Mil...	Focal islet hyperplasia.
4.239	No diabetes	Negative	41		Male	Caucasian	20.55		20.5			Ins+/Gluc+ islets. Mild adipose infiltration exocrine regions.	Scaring one section. 1 foci mononuclear infiltrate peri-vascular.

6.524	No diabetes	Negative	24.2		Male	Caucasian	1.01		24.8	IA2A+ by screening.		Ins+/Gluc+ islets. Occ. high islet Ki67.	
7.028	No diabetes	Negative	45.8		Female	Caucasian	4.45	5.6	25			Ins+/Gluc+ numerous islets, normal sizes. No infiltrates. Mild acinar fat. ...	Multifocal ductular dysplasia with epithelial proliferation. Extra-acinar islets have back ground staining of insulin into surrounding connective tissues. Minor background of DAB chromogen for CD3 too.
9.972	No diabetes	Negative	31		Female	Caucasian	6.23	5.5	26.9		Head Trauma (MVA)	Ins+/Gluc+ islets, no abnormalities observed. Occasional islet hyperemia.	
4.984	No diabetes	Negative	20		Female	Caucasian	6.89	5.8	25.6		Head trauma (MVA)	Ins+/Gluc+ islets. No abnormalities observed. Low Ki67 all compartments.	
4.153	No diabetes	Negative	31		Male	Caucasian	8.1		25.4		Head Trauma (Gun shot)	Ins+/Gluc+ islets, numerous. Occ. islet has high numbers Ki67 cells. Islet ...	Very clean pancreas, PanTail has 1 lobule with high fatty infiltration.

5.286	T1D	Negative	22.4	14	Male	Caucasian	<0.05		24.1	Maternal uncle and paternal grandfather had T1D. Retinopathy and neuropathy...		Ins-/Gluc+ islets. Mild to moderate atrophy.	Islets reasonable number and sizes.
19.345	T1D	Negative	31.4	15	Male	Hispanic	0.24		28			Ins+ islets. Mild to moderate chronic pancreatitis. Moderate interlobular a...	Ki67+ vascular smooth muscle. Mild ductular metaplasia.
7.813	T1D	GADA+ IA-2A+ ZnT8A+ mIAA+	31.2	5	Male	Caucasian	<0.05		27			Ins+/Gluc+ islets (much decreased). Insulitis. Chronic pancreatitis- mild, ...	Possible insulitis. Mild to moderate CVD. Fatty infiltrate mild. Very mild, focal autolysis few blocks. Peri-ductular fibrosis moderate.
9.615	T1D	GADA+ mIAA+	43.5	21	Male	Caucasian	<0.05		28.7	GADA+ by autoab. screening. Endstage renal failure (dialysis 1 year), HTN, ...		Ins- islets including extra-acinar. Moderate to severe exocrine atrophy. Mo...	
8.954	T1D	mIAA+	49.2	41	Female	Caucasian	<0.05		33.7	Coronary artery disease and hypertension.		Ins-/Gluc+, atrophy, decreased numbers. High acinar and duct Ki67. CD3+ inf...	At recovery noted: areas of fatty pancreas with evidence of chronic

													inflammation and pancreatitis. Admission glucose >600 and hypo-kalemia. PA also noted gross enlargement with areas of saponification and pancreatitis.
37.748	T1D	Negative	44.1	15	Male	Caucasian	<0.05		23.9			Ins-/Gluc+ islets, reduced density. Acinar atrophy moderate to severe with ...	
33.881	T1D	GADA+ mIAA+	26	15	Female	African American	0.48		26.6			Ins+ (reduced numbers but in all regions)/Gluc+ islets, normal sizes, reduc...	Possible amyloid.
51.234	T1D	GADA+ mIAA+	28	21	Male	Caucasian	<0.05	7.2		Mother had gestational diabetes while pregnant with donor. Hypertension (mi...		Ins-/Gluc+ islets. High duct and exocrine Ki67. Small duct plugging with ru...	Some black precipitate may interfere with image analysis. Acute and chronic pancreatitis.
75.039	T1D	Negative	32	16	Female	Caucasian	<0.05		23.4			Ins-/Gluc+ islets present in reduced numbers. No significant inflammation b...	

6.925	T1D	GADA+ mIAA+	35	11	Female	Caucasian	<0.05		27.4		Anoxia	Ins-/Gluc+ islets in much reduced numbers. Moderate widespread exocrine atr...	
11.819	T1D	mIAA+	61	52	Male	Caucasian	<0.05		21.6		Cerebro vascular/Stroke	Ins-/Gluc+ islets (pseudoatrophic). Exocrine atrophy moderate with focal mi...	Reviewed with Chen Liu- PanIN1 designation. Stretch to call PanIN2.
49.447	T1D	Negative	58	22	Female	Caucasian	1.28	6.1	28.6		Not avail	Ins+/Gluc+ islets (much reduced numbers). Severe chronic pancreatitis. Mode...	Chen Liu reviewed 8/16/13 mct. Also reviewed 3/24/14 1. Tremendous atrophy. 2. Lots of islets. 3. Insulin+ islets- lots. 4. PanIN2- PT 04, focal. T2D likely.
9.848	T1D	IA-2A+ mIAA+	39	19	Male	Caucasian	<0.05		19.5	Fell (non-MVA accident).	Head Trauma	Ins-/Gluc+ islets. Acute pancreatitis- moderate to focally severe. Duct plu...	Chen Liu reviewed 8/16/13 mct.
16.588	T1D	IA-2A+	41	27	Female	African American	<0.05		21.1		Cerebro vascular/Stroke	Ins-/Gluc+ islets in reduced numbers. Extra-acinar islets in fibrotic regio...	A*36:01 , 74:01

16.744	T2D	Negative	18.8	0.25	Female	Hispanic	10.68		39.1	DKA 3 months prior with acute renal failure. 3 months duration diabetes. Ca...		Ins+ islets, clusters, single cells plentiful. CD3+ foci intra-acinar and p...	Islets are insulin + with normal Ki67 (ie, rare). Ducts have normal numbers of beta cells (present yet exceedingly low proportion). Only occ. focal ductular proliferation or mucinous metaplasia. Glucagon + islet cells very heterogeneous distribution between lobules and faint. Fatty infiltrate mild-note high BMI.
9.384	T2D	mIAA+	48.8	0	Female	Hispanic	<0.05	8	32.5	Preclinical. Plasma (no serum) available.		Ins+/Gluc+ islets though in reduced density, especially in head. Amyloid. L...	Mild autolysis PanHead 02. Islets in head region arranged more in loops compared to body and tail regions.
12.470	T2D	Negative	20.7	0	Female	African American	0.58		40	Acute onsent. Gestational diabetes in past. Father		Ins+ (reduced)/Gluc+ islets various sizes, some	Some lobules have increased fibrosis between acinar cells.

										had diabetes.		atrophied. Low Ki67. No fat...	
16.204	T2D	Negative	42.8	2	Male	Caucasian	0.58	7.8	31	Diabetes medication was oral Metformin (1 g/day) for 2 years but noncomplia...		Ins+ (reduced)/Gluc+ islets with severe amyloidosis. Severe exocrine atroph...	Megaislets/islet hypertrophy (8/26/13)
7.236	T2D	Negative	62.3	3	Male	Caucasian	2.85		33.7	Metformin for 3 years.		Ins+/Gluc+, normal islet density. Hypertrophied islets. Amyloid. Acinar atr...	Mild acinar autolysis with possible secondary changes connective tissues including islet vasculature. Islet hypertropy.
1.478	T2D	mIAA+	44.8	10	Female	Caucasian	0.08		30.4			Ins+ (reduced)/Gluc+ islets. Mild adiposity exocrine regions. Low Ki67.	Amyloid noted 5/30/13 mct.
6.195	T2D	Negative	55.8	0	Female	Hispanic	0.8	9.1	44.6	Preclinical T2D ie no diagnosis or medication for diabetes; Hypertension fo...		Ins+ (reduced) islets, numerous, smaller. Low Ki67. Amyloid. Exocrine atrop...	

45.791	T2D	No serum available	45.1	20	Male	Hispanic	No serum available	8	25.3	No serum or cells available. Negative for GADA and IA2A by autoantibody scr...		Ins+ (weak)/Gluc+ islets, numerous but small sized. Mild acinar atrophy.	HbA1c added mct 7/22/13
7.641	T2D+Incretin	Negative	68.3	5	Male	Caucasian	2.98	6.3	20.9			Ins+/Gluc+ islets, plentiful; mild, multifocal amyloid. Mild, multifocal ch...	Low Ki67. HbA1c added mct 7/22/13
24.893	T2D	Negative	36.1	0	Male	Hispanic	3.45	7.2	30.6	Preclinical T2D based on HbA1c.		Ins+/Gluc+ islets. Low Ki67. No infiltrates or amyloid observed.	
15.458	T2D+Incretin	mIAA+	48.5	26	Female	Caucasian	1.85		36.1			Ins+/Gluc+ numerous islets. Rare amyloid in islets. Very mild chronic pancr...	Focally severe exocrine atrophy.
29.407	T2D	Negative	62	10	Female	Caucasian	6.14	6	19.9	Metformin 1g / twice a day.		Ins+/Gluc+ plentiful islets, several with vascular congestion or amyloid. S...	
11.393	T2D+Incretin	Negative	47.4	13	Male	Caucasian	0.16	7.3		Renal tranplant 7 years ago; retinopathy.		Ins+/Gluc+ islets, numerous. Moderate acinar atrophy with fatty replacement...	IPMN PanHead 04 block (this statement added to histopath and specimen levels 1/14/14 mct)

24.064	**T2D+Incretin**	**Negative**	**53**	**20**	**Male**	**African American**	**8.87**		**29.6**	**Father and 3 siblings with diabetes.**		**Ins+/Gluc+ islets with moderate fibrosis and variable amyloidosis. Moderate...**	

Supplementary Figure legends

Fig. S1. Generation of conditional and constitutive *Fap* Ser624Ala knockin (FAPgki) mice. Representation of the *Fap* wildtype genomic locus (A), the targeted locus Fap^{flox} (B), the FRT recombined locus Fap^{conKI} (C) and the *Cre* deleted locus Fap^{KI} (D). 5' probe, 3' probe, enP probe and relevant restriction sites are indicated, as well as the positions of the wildtype *Fap* mini cDNA cassette and *PGK-neomycin* selection cassette.

Fig. S2. Southern blot verification of $Fap^{wt/conKI}$ and $Fap^{wt/KI}$ mice. Southern blot screening tail DNA confirmed targeted recombination at each end of the Fap locus: 5' probe on *Eco*RV digest showing Fap^{wt} and Fap^{flox} alleles (A), 3' probe on *Kpn*I digest showing Fap^{wt} and Fap^{flox} alleles (B). Fap^{conKI} (C) and Fap^{KI} alleles (D) were identified using the enP probe on *Eco*RV digest. The use of a neomycin probe confirmed a single integration event (data not shown). As expected, intrahepatic *Fap* gene expression levels were comparable in WT and $Fap^{KI/KI}$ mice (E).

Fig. S3. FAPgki mice lacked FAP enzyme activity but retained cell surface expression of FAP protein. (A) FAP specific enzyme assay of plasma from 3-week-old mice showed that **$Fap^{KI/KI}$ (FAPgki)** mice lacked FAP enzyme activity whereas **$Fap^{wt/KI}$** mice had approximately half as much FAP enzyme activity as WT mice (n=2 mice per group). (B) Flow cytometry on primary lung fibroblasts from a FAPgki mouse showed that the single point mutation at the enzyme active site serine did not prevent cell surface expression of FAP (30.9% FAP positive cells) in the FAPgki mice . (C) Clockwise flow cytometry gating strategy showed that live and single cells were gated to identify the percentage of FAP positive cells, compared with IgG control. Histogram key: blue is control IgG, red is anti-FAP.

Fig S4. Improved glucose tolerance in male FAP gko mice. Oral GTT (A) and glucose AUC (B) at 14 weeks of HFD (Specialty Feeds). Ip GTT (C) and glucose AUC (D) at 20 weeks of HFD (in-house HFD). Individual replicates (B, D). Mean ± SEM. n = 6 male mice per group. *$p<0.05$ by Mann-Whitney U test.

Fig. S5. FAPgki mice were protected from pancreatic islet hypertrophy. FAPgki and WT male mice following 12 weeks of in-house HFD. Representative islets of those quantified for the data presented in Figure 3, immunostained for insulin and glucagon.

Fig. S6. FAP gko mice were resistant to HFD induced steatosis. Intrahepatic lipid measured by quantitative calorimetric oil red O assay (fold change from average of WT Chow). Liver was obtained after overnight fasting. *$p<0.05$, with or without exclusion of the highest data point, versus genotype-matched controls using Mann-Whitney U test. Individual replicates and mean ± SEM. n=5-6 female mice per group. Fold changes from livers depicted in Fig. 4 panels E and F were, respectively, 257% and 206%.

Fig. S7. FAP gko mouse liver. Sirius Red staining did not detect fibrosis in either WT (A) or FAP gko (B) mice. Representative liver sections from n=5-6 female mice per group, at 20 weeks of HFD (in-house diet). Scale bars= 200 μm.

Fig. S8. F4/80 macrophage stain in liver and adipose tissue. Liver (A), BAT (C), WAT (D) with immunoperoxidase stain of F4/80 and haematoxylin counterstain for nuclei. Quantitation of immunopositivity in liver as a percentage of area in 5 fields at x200 magnification from 5 mice per group (B). Scale bars = 100 μm.

Fig. S9. FAP deficient mice were resistant to HFD induced obesity. Change in live body weight following the start of diet (A, C) and autopsy body weight at 20 weeks of diet (HFD; Specialty Feeds) in WT and FAP gko mice (B) and 17 weeks of in-house HFD in WT and FAPgki mice (D). Individual replicates (A, C). Mean ± SEM. n = 10-12 female (A, B) or 12-14 male (C, D) mice per group. *$p<0.05$ versus genotype-matched controls using Mann-Whitney U test.

Fig. S10. Glucose tolerance AUC was not correlated with body weight or adiposity in FAP deficient mice. Regression analysis of GTT AUC versus body weight (A) or adiposity (total fat pad weight : body weight; B) of WT and FAP gko mice. Regression analysis of

GTT AUC versus body weight of WT and FAPgki mice (C). These data derive from 20 weeks of in-house HFD. Scatter plots show individual replicates and line of best fit. n=10-12 female (A, B) or 5 male (C) mice.

Fig. S11. Circulating active GLP-1 and intrahepatic *Pparα* and *Srebp1c* mRNA were unaltered by FAP deficiency in mice. GLP-1 (7-36) levels in plasma following overnight fasting (basal) and at 15 minutes after a glucose challenge at 20 weeks of diet (A). mRNA expression of *Pparα* (B, D) and *Srebp1c* (C, E) relative to 18S house keeping gene at 20 weeks of HFD. Individual replicate mice. Mean ± SEM. n=5-6 female (A), or n=10-12 female (B, C) or male (D, E) mice per group.

Fig. S12. Intrahepatic mRNA expression of *Dpp4* gene family members was not altered in FAP gko mice compared to WT mice. Transcripts relative to housekeeper gene *18S* RNA. n=10-12 female mice per group, fed either chow (A) or HFD (B) for 20 weeks. Individual replicate mice.

Fig. S13. *Dpp9* expression and its association with *Dpp4* and *Chrebp* expression. *Dpp9 mRNA* expression was downregulated in HFD mice compared to chow mice (A), and was correlated with *Dpp4* (B) and *Chrebp* mRNA (C), regardless of mouse genotype. Transcripts relative to housekeeper gene *18S*. Basal mRNA expression from overnight fasted mice. n=10-12 female mice per group. Scatter plots show individual replicates (A-C). Mean ± SEM (A). Line of best fit for each genotype (B, C). *$p<0.05$ by Mann-Whitney U test.

Fig. S14. CD36 immunopositivity in hepatocytes was less in FAPgki than WT liver. Immunofluorescence of CD36 on mouse liver sections, with immunopositivity from cells having morphological characteristics of hepatocytes and macrophages (A). Quantitation of four fields per section at 200x magnification in arbitrary units of total intensity of fluorescent signal at 488 nm absorbance. Scale bars = 30 μm.

Fig. S15. FAP depletion was not associated with changes in physical activity or energy expenditure. Physical activity (A) and energy expenditure (B) were measured by indirect calorimetry at 12 weeks of HFD (in-house diet). Mean ±SEM, n=6-8 female mice per group. *p<0.05 versus genotype-matched controls using Mann-Whitney U test.

Fig S16. Proposed model of effects of FAP deficiency in mice. Effects of FAP implied from these studies of FAP deficient mice, pathways of FAP action that were identified, and molecules that are potentially involved.

Supplementary Material References

[1] Wang XM, Yu DMT, McCaughan GW, Gorrell MD. Fibroblast activation protein increases apoptosis, cell adhesion and migration by the LX-2 human stellate cell line. Hepatology 2005;42:935-945.
[2] Keane FM, Yao T-W, Seelk S, Gall MG, Chowdhury S, Poplawski SE, et al. Quantitation of fibroblast activation protein (FAP)-specific protease activity in mouse, baboon and human fluids and organs. FEBS Open Bio 2014;4:43-54.
[3] Osborne B, Yao T-W, Wang XM, Chen Y, Kotan LD, Nadvi NA, et al. A rare variant in human fibroblast activation protein associated with ER stress, loss of function and loss of cell surface localisation. Biochim Biophys Acta 2014;1844:1248-1259.
[4] Lo L, McLennan SV, Williams PF, Bonner J, Chowdhury S, McCaughan GW, et al. Diabetes is a progression factor for hepatic fibrosis in a high fat fed mouse obesity model of non-alcoholic steatohepatitis. J Hepatol 2011;55:435-444.
[5] Henderson JM, Polak N, Chen J, Roediger B, Weninger W, Kench JG, et al. Multiple liver insults synergize to accelerate experimental hepatocellular carcinoma. Scientific Reports 2018;8:10283.

Supplementary Material

Fibroblast activation protein enzyme deficiency prevents liver steatosis, insulin resistance and glucose intolerance and increases fibroblast growth factor-21 in diet induced obese mice

Sumaiya Chowdhury, Sunmi Song, Hui Emma Zhang, Xin Maggie Wang, Margaret G. Gall, Denise Ming Tse Yu, Angelina J. Lay, Michelle Sui Wen Xiang, Kathryn A. Evans, Stefanie Wetzel, Yolanda Liu, Belinda Yau, Andrew L. Coppage, Lisa Lo, Rebecca A. Stokes, Wayne J. Hawthorne, Gregory J. Cooney, Susan V. McLennan, Jenny E. Gunton, William W. Bachovchin, Nigel Turner, Melkam A. Kebede, Geoffrey W. McCaughan, Stephen M. Twigg, Mark D. Gorrell

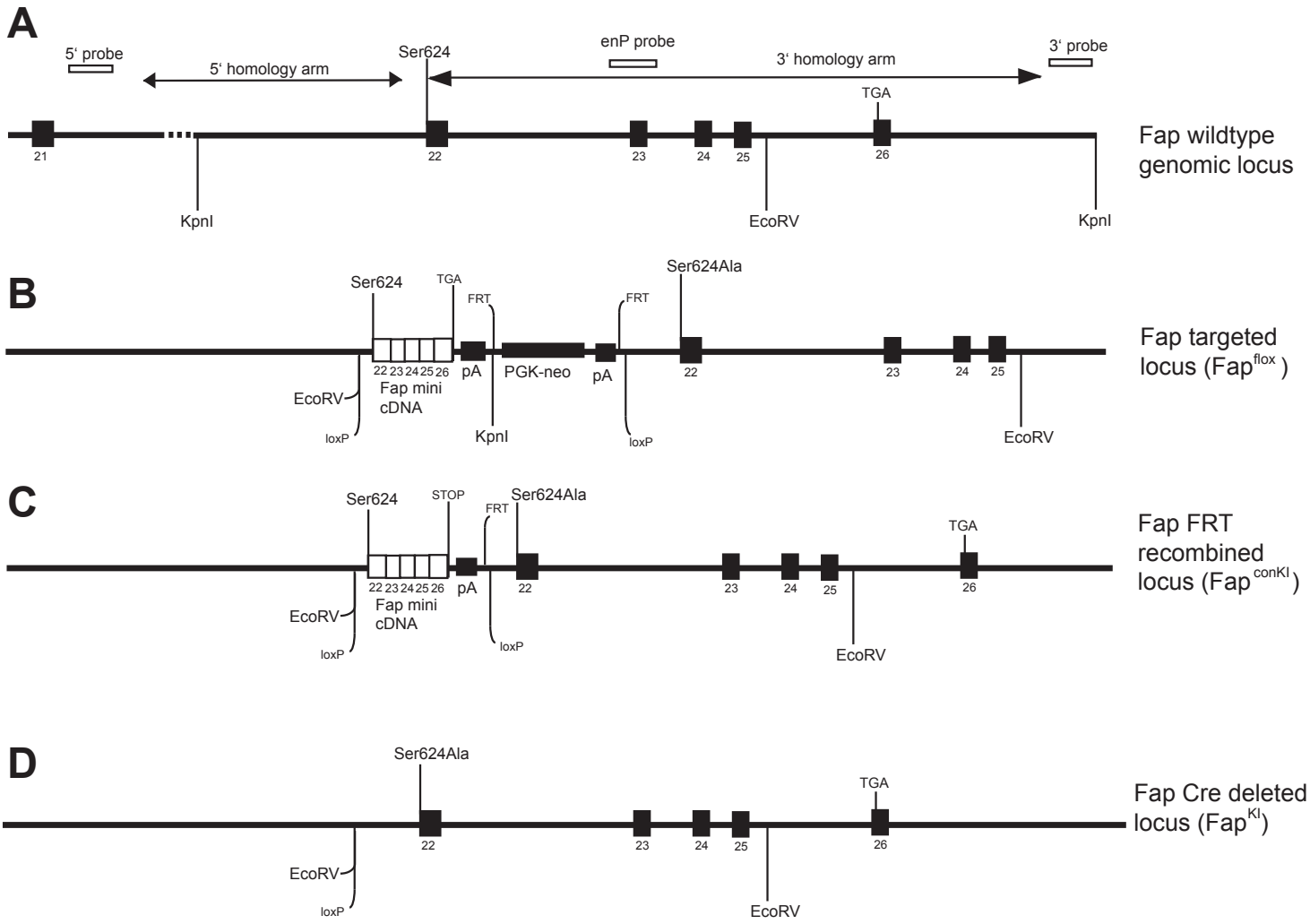
A
5' probe
5' homology arm
Ser624
enP probe
3' homology arm
3' probe
TGA
21
22
23
24
25
26
KpnI
EcoRV
KpnI
Fap wildtype genomic locus
B
Ser624
TGA
FRT
FRT
Ser624Ala
22 23 24 25 26
pA
PGK-neo
pA
Fap mini cDNA
EcoRV
loxP
KpnI
loxP
22
23
24
25
EcoRV
Fap targeted locus (Fap flox)
C
Ser624
STOP
FRT
Ser624Ala
TGA
22 23 24 25 26
pA
22
23
24
25
26
Fap mini cDNA
EcoRV
loxP
loxP
EcoRV
Fap FRT recombined locus (Fap conKI)
D
Ser624Ala
TGA
22
23
24
25
26
EcoRV
loxP
EcoRV
Fap Cre deleted locus (Fap KI)

Fig. S1

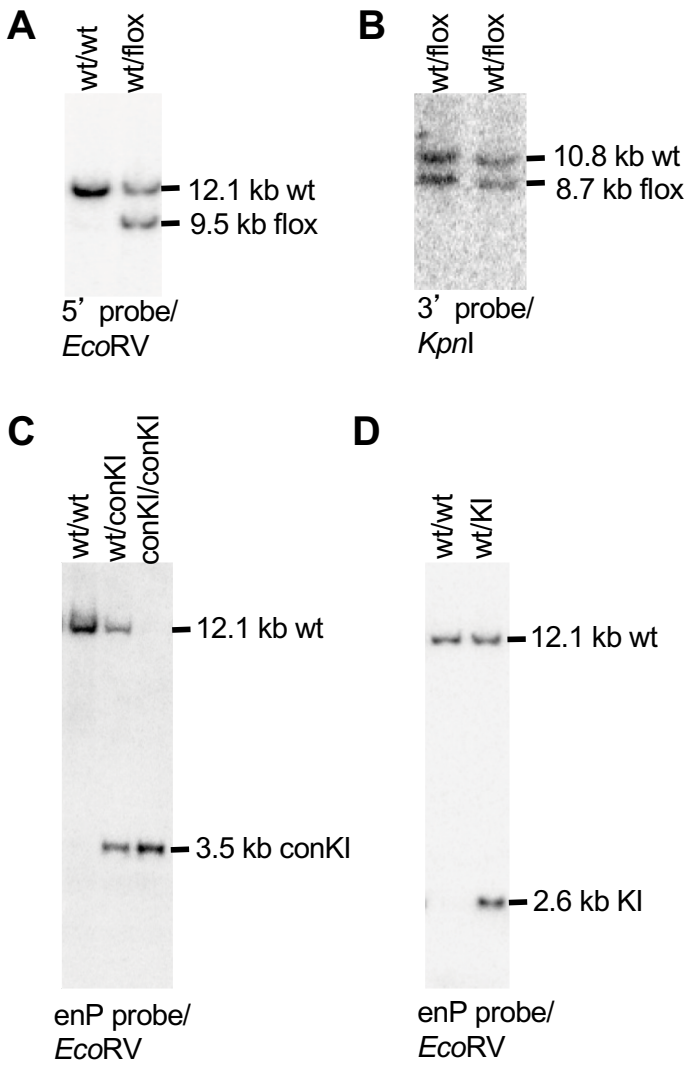
A
wt/wt
wt/flox
12.1 kb wt
9.5 kb flox
5' probe/
EcoRV
B
wt/flox
wt/flox
10.8 kb wt
8.7 kb flox
3' probe/
KpnI
C
wt/wt
wt/conKI
conKI/conKI
12.1 kb wt
3.5 kb conKI
enP probe/
EcoRV
D
wt/wt
wt/KI
12.1 kb wt
2.6 kb KI
enP probe/
EcoRV
E
Fap
Relative expression
2.5
2.0
1.5
1.0
0.5
0.0
WT
FAP gki

Fig. S2

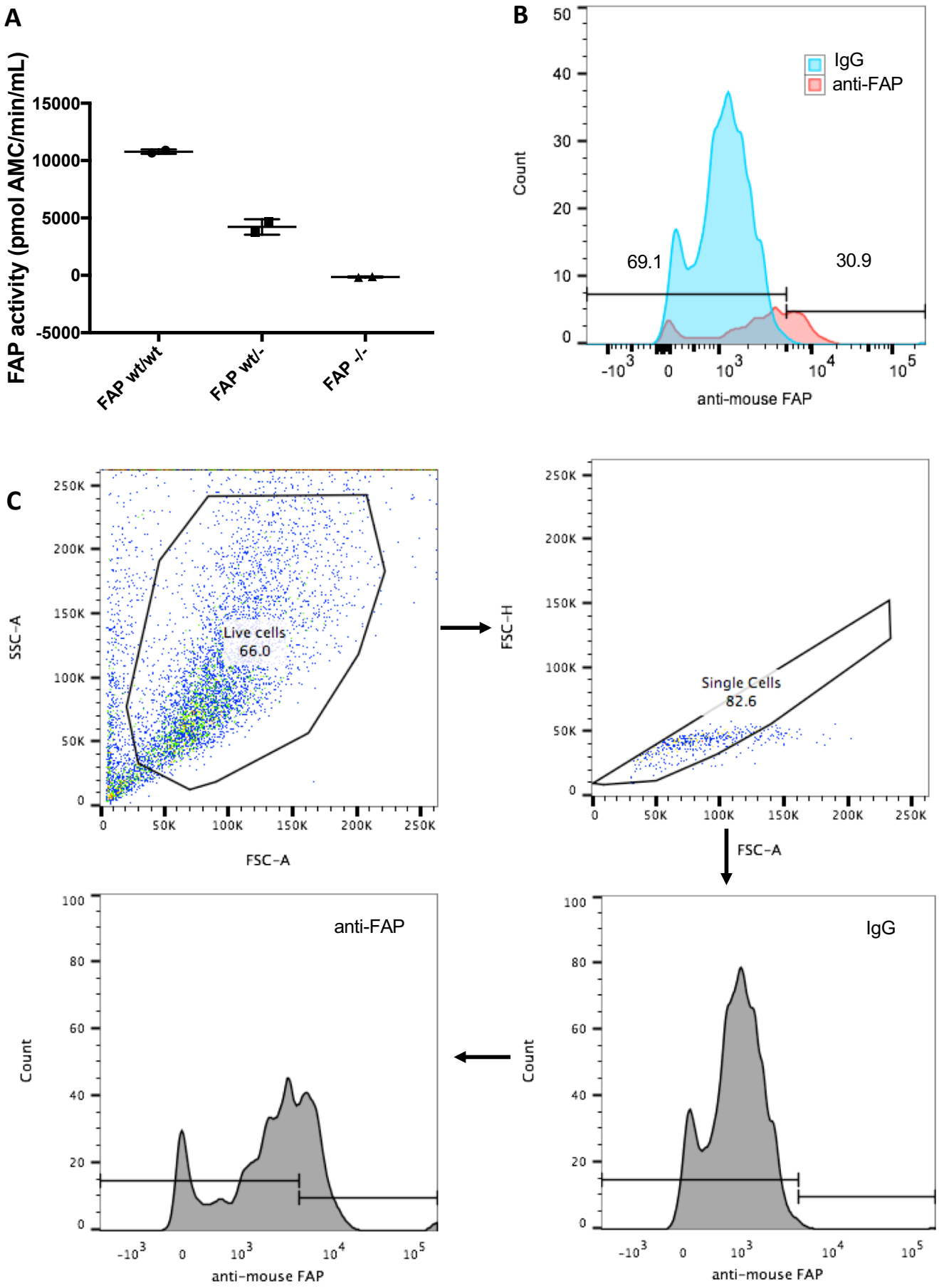
A
FAP activity (pmol AMC/min/mL)
15000
10000
5000
0
-5000
FAP wt/wt
FAP wt/-
FAP -/-
B
IgG
anti-FAP
Count
69.1
30.9
anti-mouse FAP
C
SSC-A
Live cells
66.0
FSC-A
FSC-H
Single Cells
82.6
FSC-A
anti-FAP
IgG
Count
anti-mouse FAP

Fig. S3

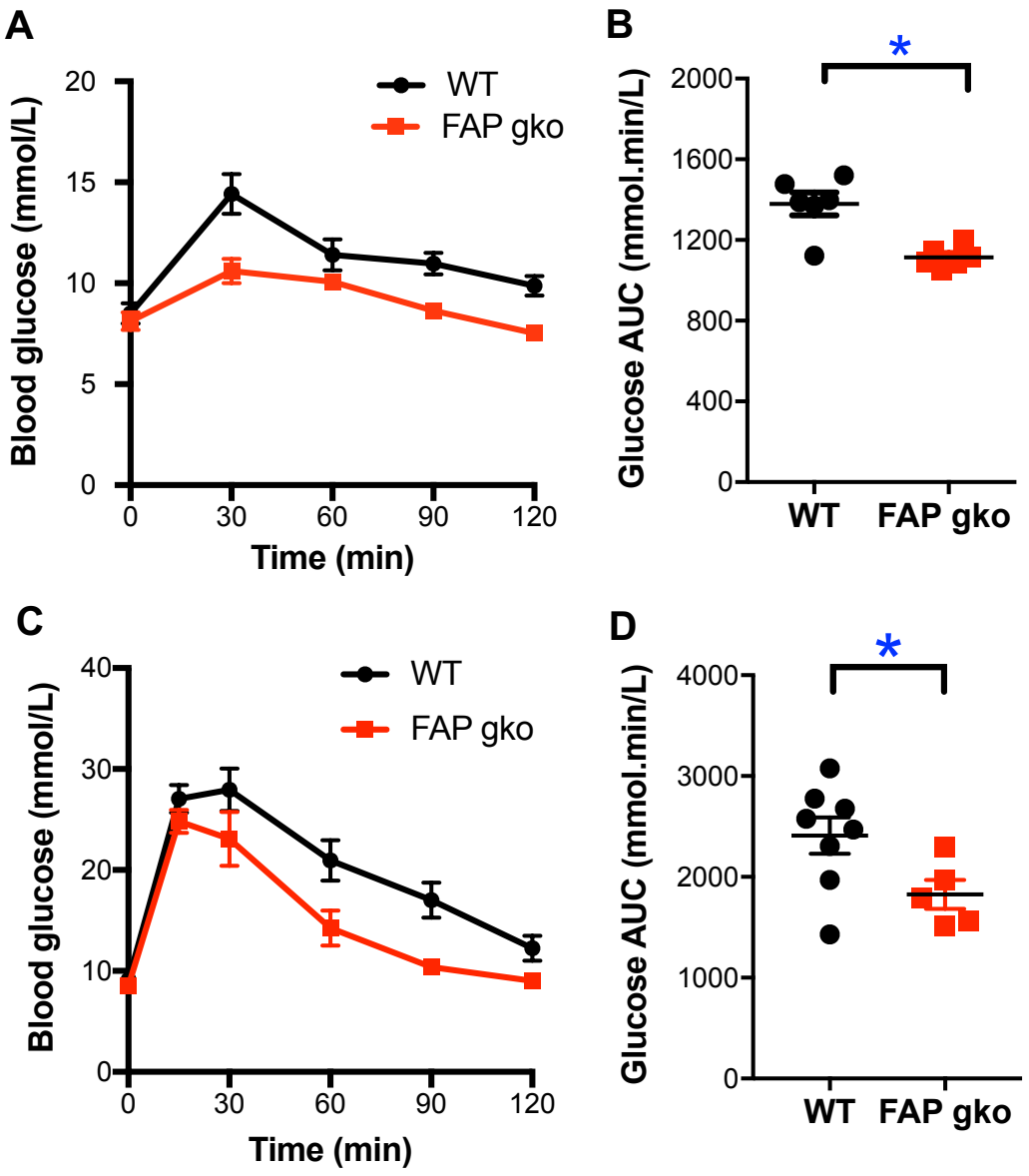
A
B
C
D
WT
FAP gko
Blood glucose (mmol/L)
Time (min)
Glucose AUC (mmol.min/L)
*
0
5
10
15
20
30
40
400
800
1200
1600
2000
3000
4000
1000
30
60
90
120

Fig. S4

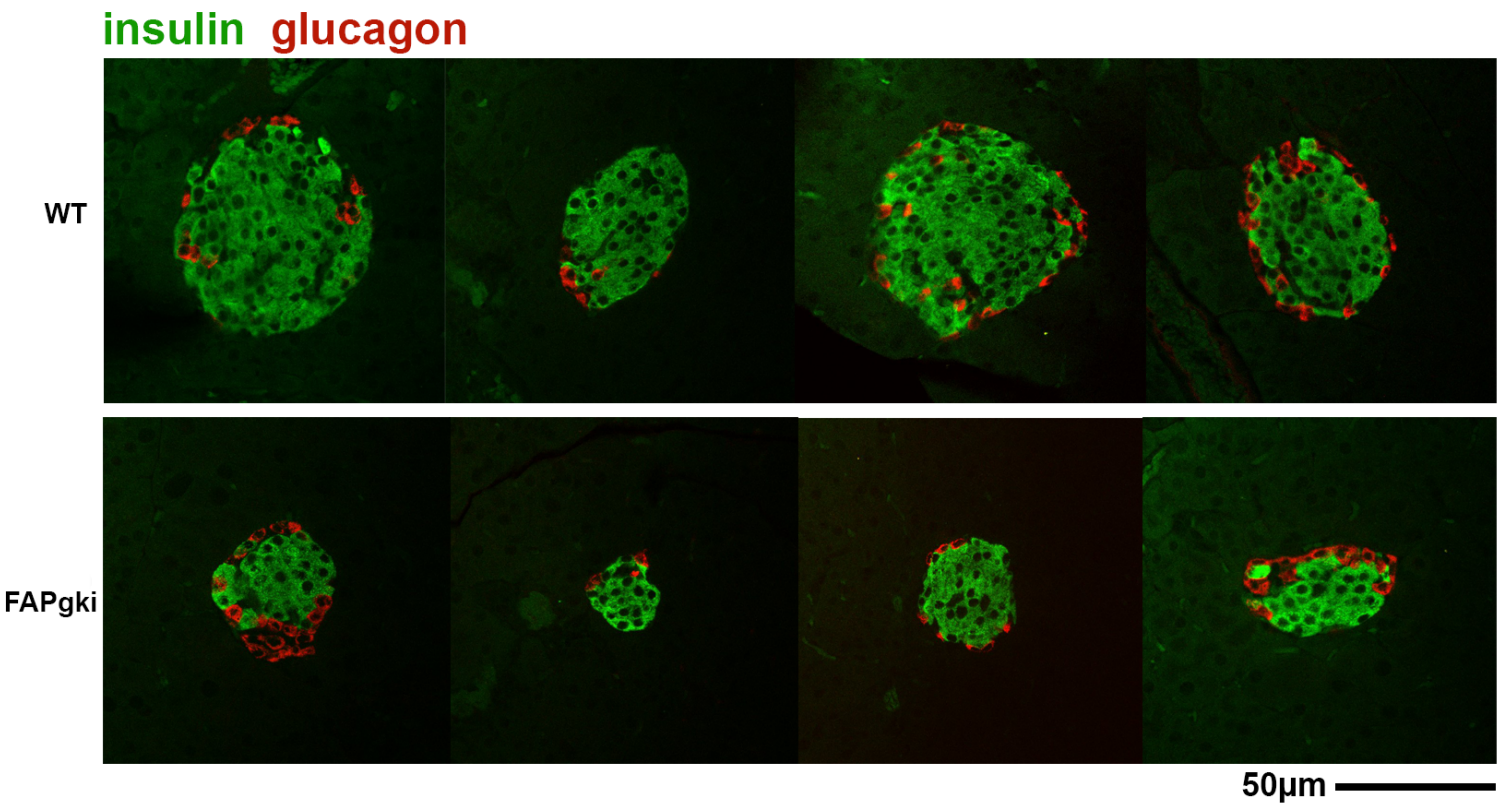

Fig. S5

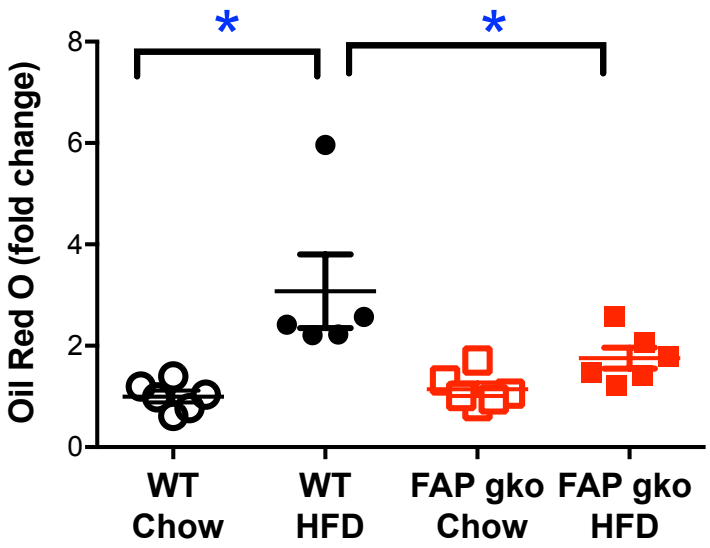
*
*
Oil Red O (fold change)
8
6
4
2
0
WT Chow
WT HFD
FAP gko Chow
FAP gko HFD

Fig. S6

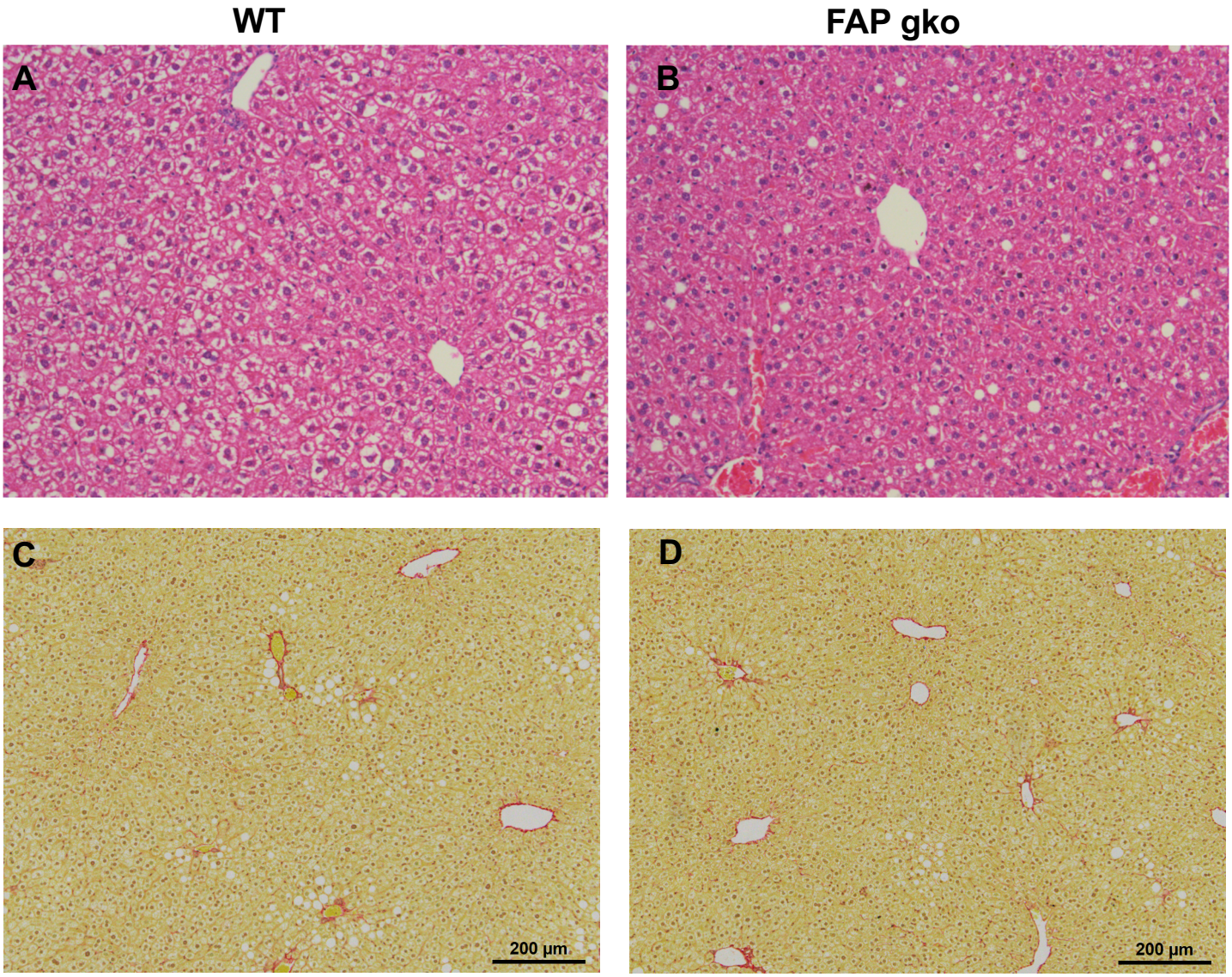

Fig. S7

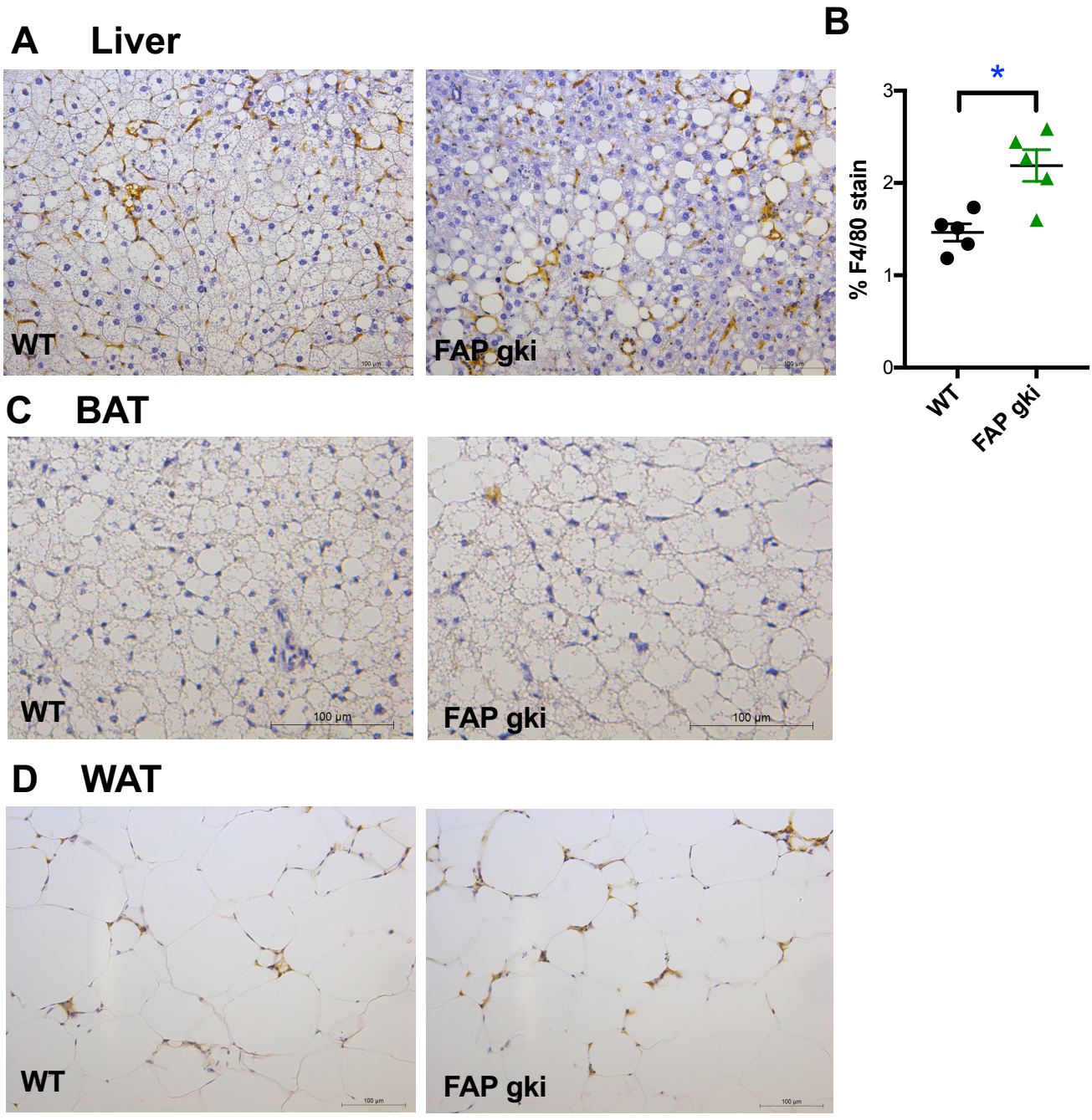
A Liver
WT
FAP gki
B
% F4/80 stain
0
1
2
3
*
WT
FAP gki
C BAT
WT
100 µm
FAP gki
100 µm
D WAT
WT
FAP gki

Fig. S8

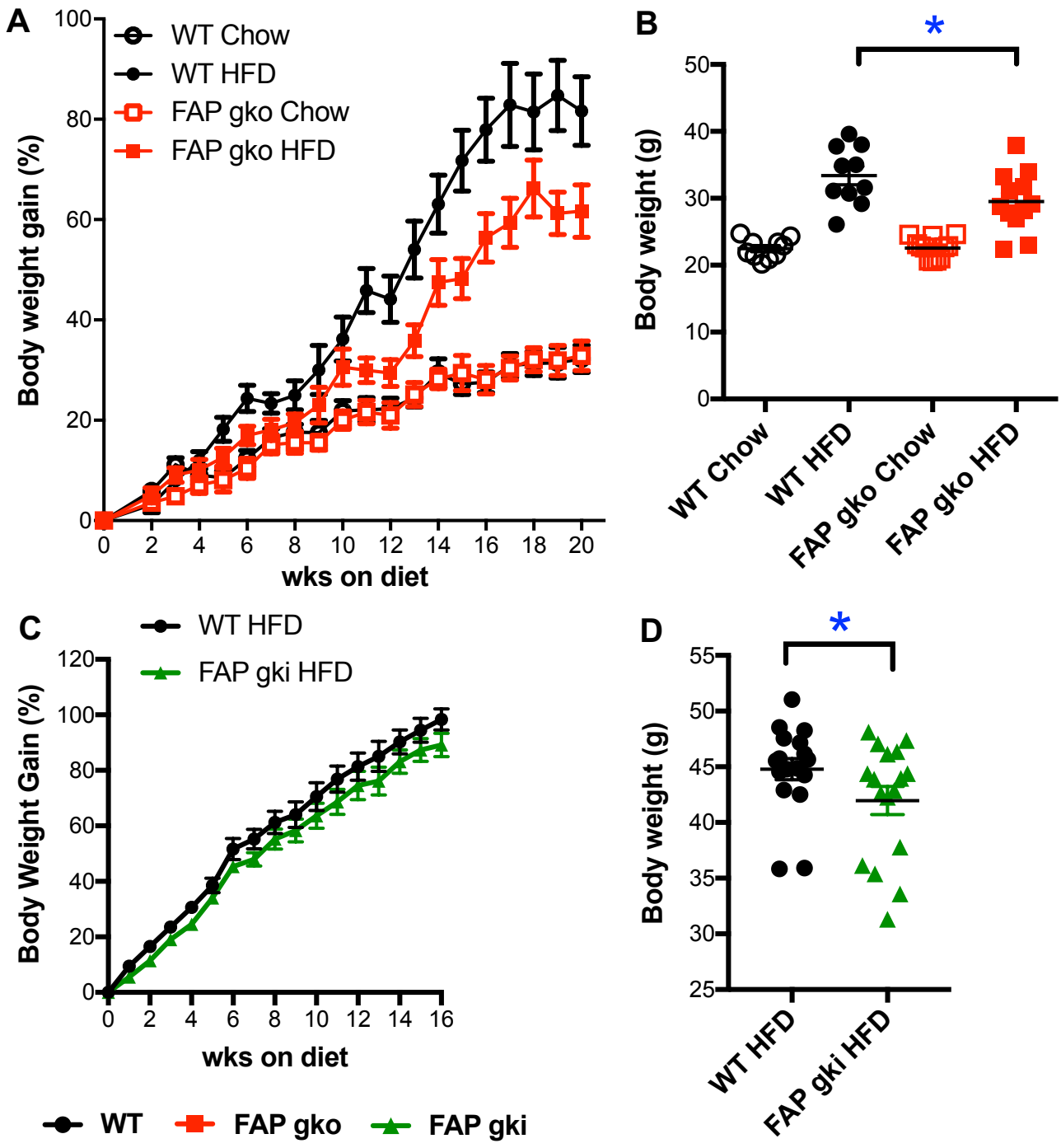
A
WT Chow
WT HFD
FAP gko Chow
FAP gko HFD
Body weight gain (%)
wks on diet
B
Body weight (g)
WT Chow
WT HFD
FAP gko Chow
FAP gko HFD
C
WT HFD
FAP gki HFD
Body Weight Gain (%)
wks on diet
WT
FAP gko
FAP gki
D
Body weight (g)
WT HFD
FAP gki HFD

Fig. S9

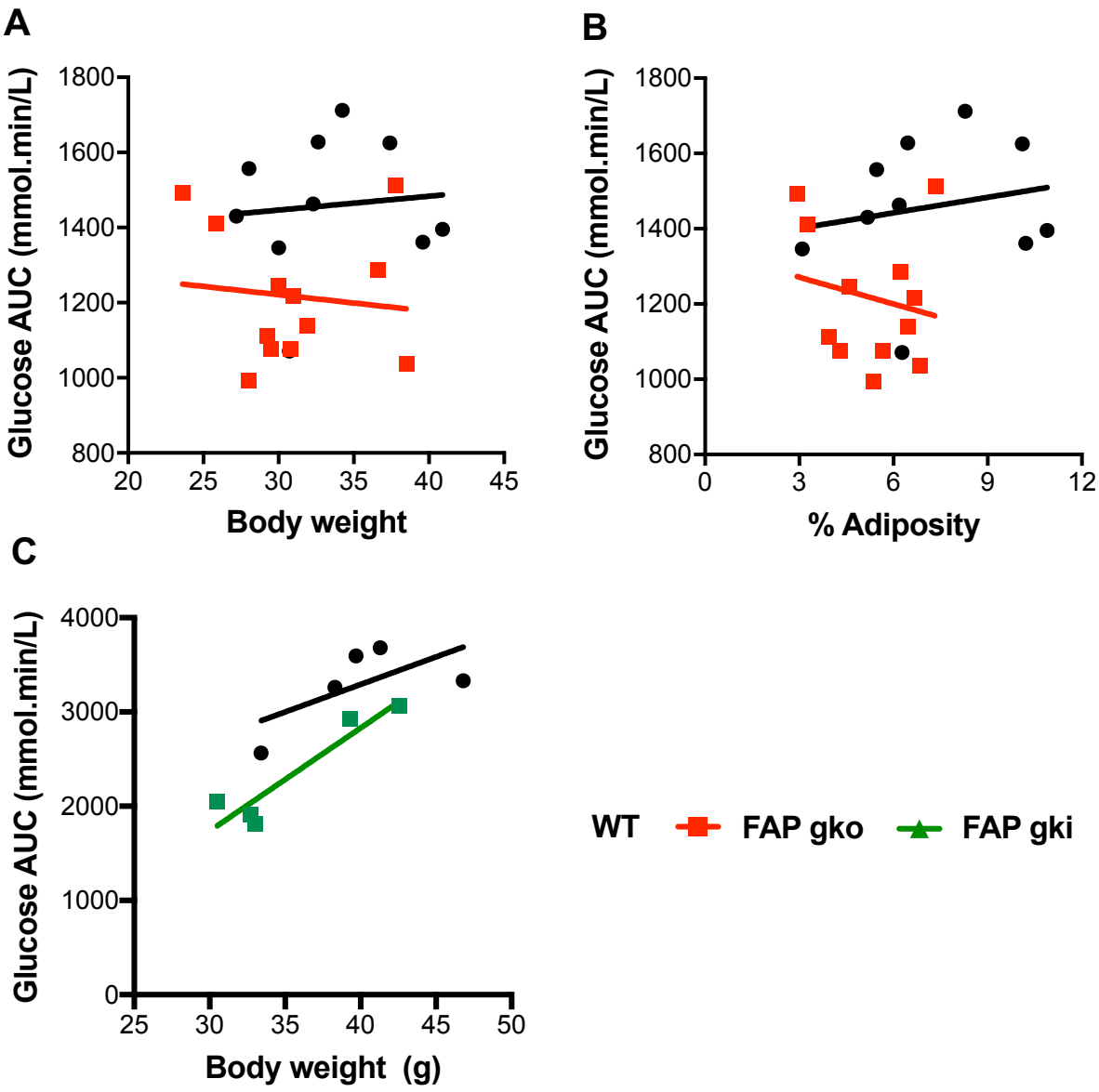
A
Glucose AUC (mmol.min/L)
1800
1600
1400
1200
1000
800
20
25
30
35
40
45
Body weight
B
Glucose AUC (mmol.min/L)
1800
1600
1400
1200
1000
800
0
3
6
9
12
% Adiposity
C
Glucose AUC (mmol.min/L)
4000
3000
2000
1000
0
25
30
35
40
45
50
Body weight (g)
WT
FAP gko
FAP gki

Fig. S10

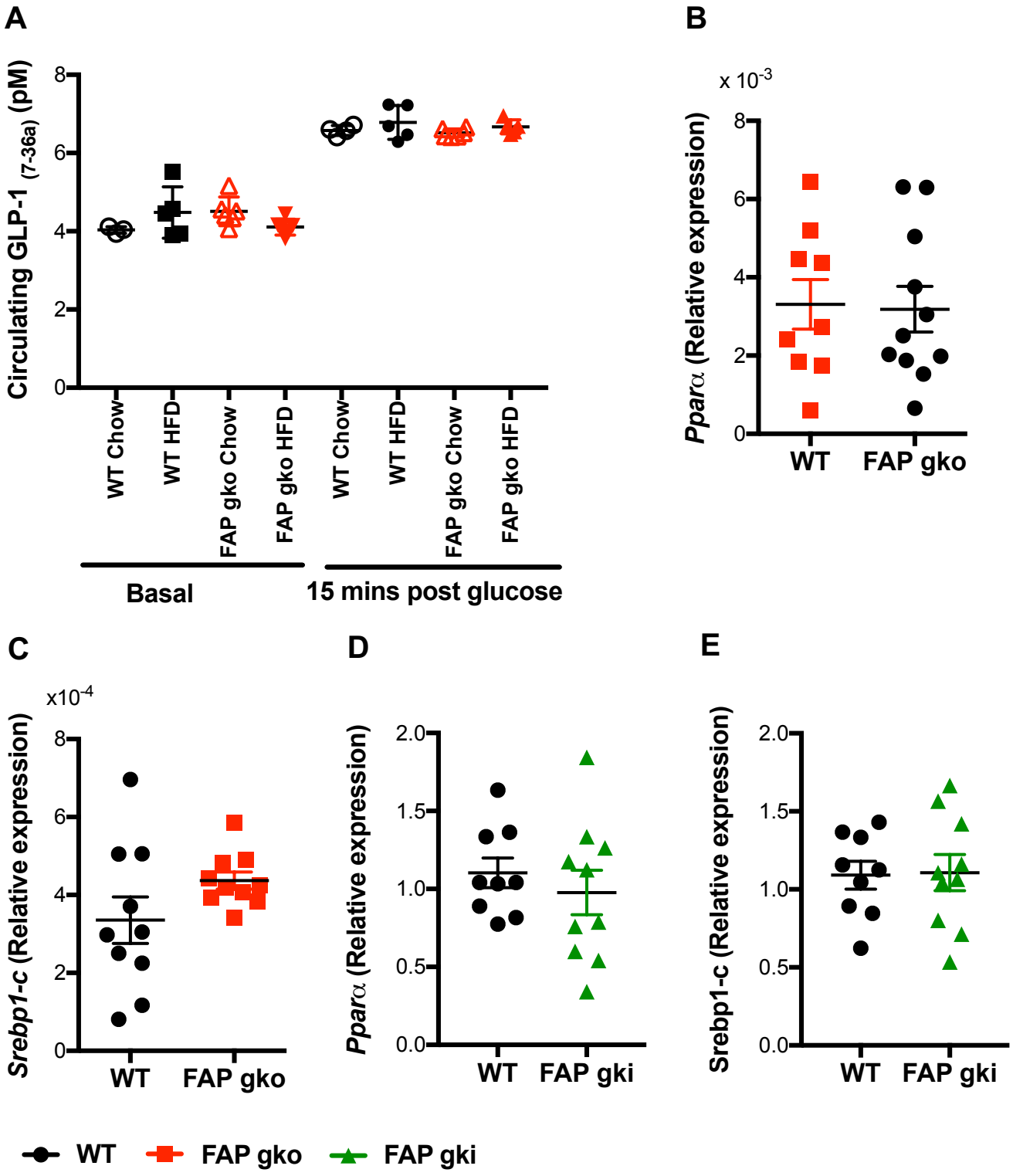
A
Circulating GLP-1 (7-36a) (pM)
8
6
4
2
0
WT Chow
WT HFD
FAP gko Chow
FAP gko HFD
WT Chow
WT HFD
FAP gko Chow
FAP gko HFD
Basal
15 mins post glucose
B
x 10-3
Pparα (Relative expression)
8
6
4
2
0
WT
FAP gko
C
x10-4
Srebp1-c (Relative expression)
8
6
4
2
0
WT
FAP gko
D
Pparα (Relative expression)
2.0
1.5
1.0
0.5
0.0
WT
FAP gki
E
Srebp1-c (Relative expression)
2.0
1.5
1.0
0.5
0.0
WT
FAP gki
WT
FAP gko
FAP gki

Fig. S11

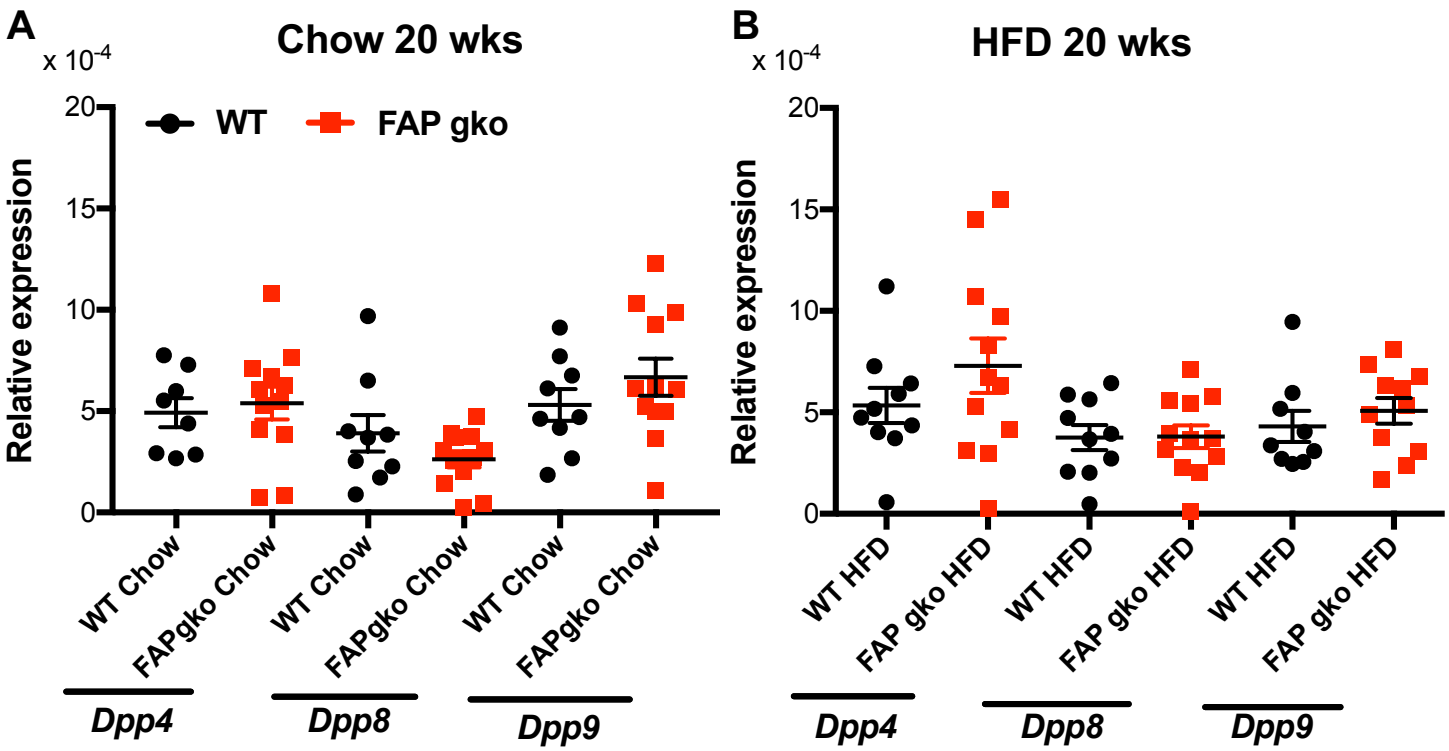
A
Chow 20 wks
x 10-4
WT
FAP gko
Relative expression
20
15
10
5
0
WT Chow
FAPgko Chow
WT Chow
FAPgko Chow
WT Chow
FAPgko Chow
Dpp4
Dpp8
Dpp9
B
HFD 20 wks
x 10-4
Relative expression
WT HFD
FAP gko HFD
WT HFD
FAP gko HFD
WT HFD
FAP gko HFD
Dpp4
Dpp8
Dpp9

Fig. S12

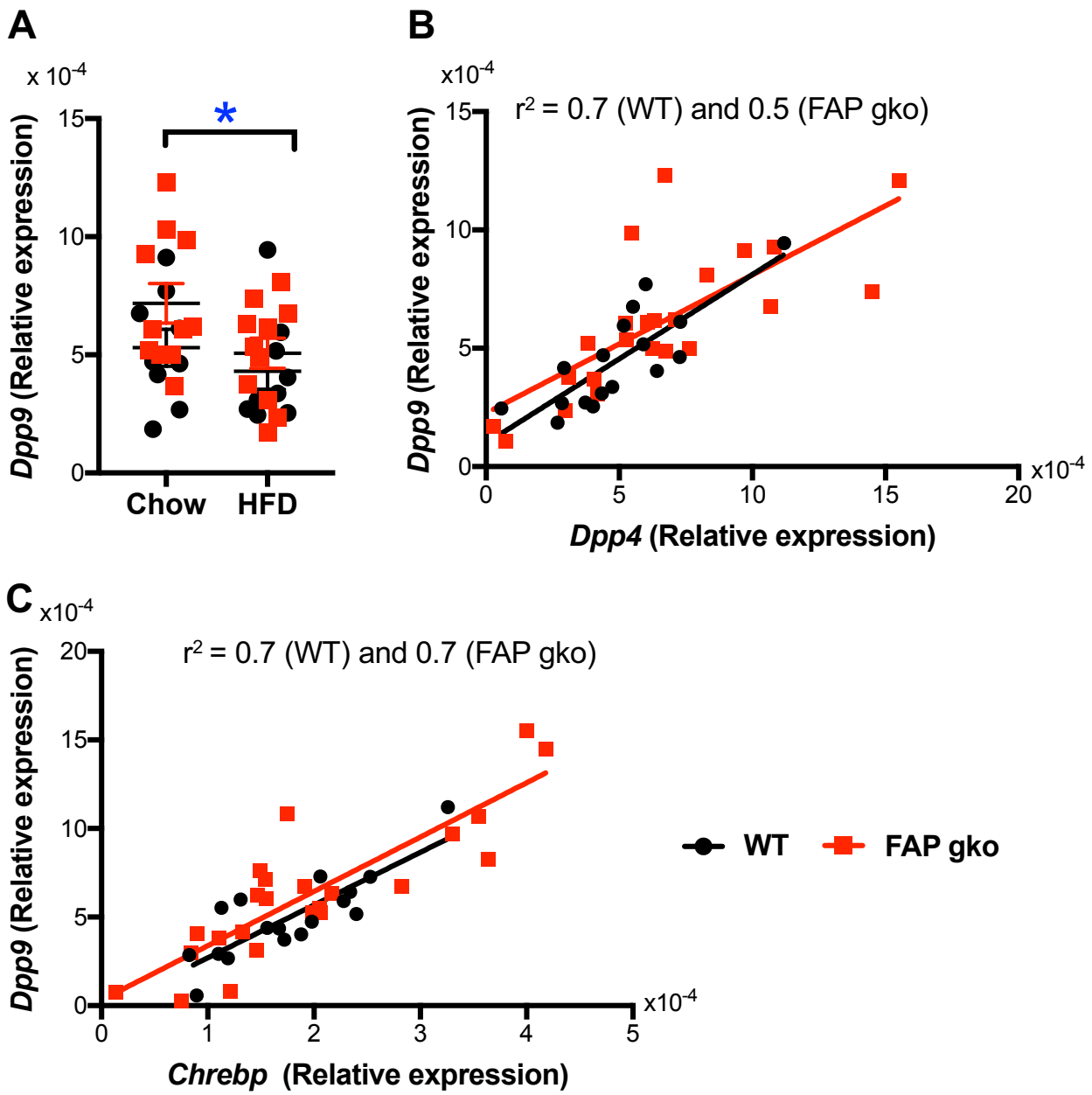
A
x 10-4
15
10
5
0
*
Dpp9 (Relative expression)
Chow
HFD
B
x10-4
r2 = 0.7 (WT) and 0.5 (FAP gko)
Dpp9 (Relative expression)
0
5
10
15
20
x10-4
Dpp4 (Relative expression)
C
x10-4
r2 = 0.7 (WT) and 0.7 (FAP gko)
Dpp9 (Relative expression)
WT
FAP gko
x10-4
Chrebp (Relative expression)

Fig. S13

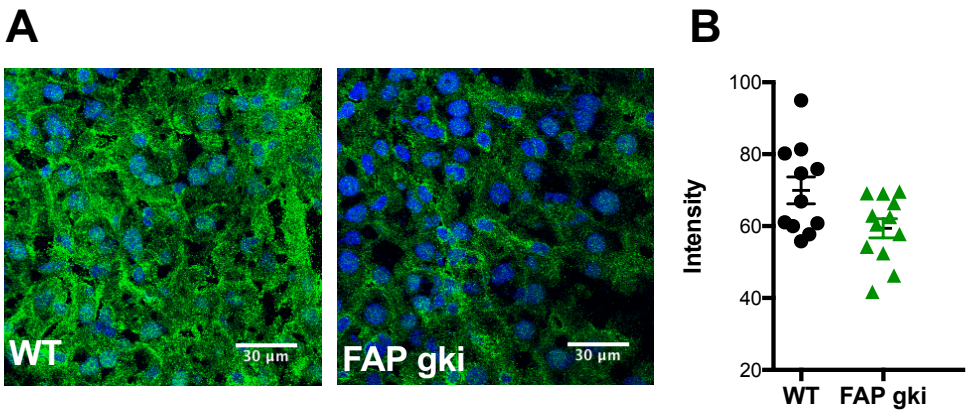

Fig. S14

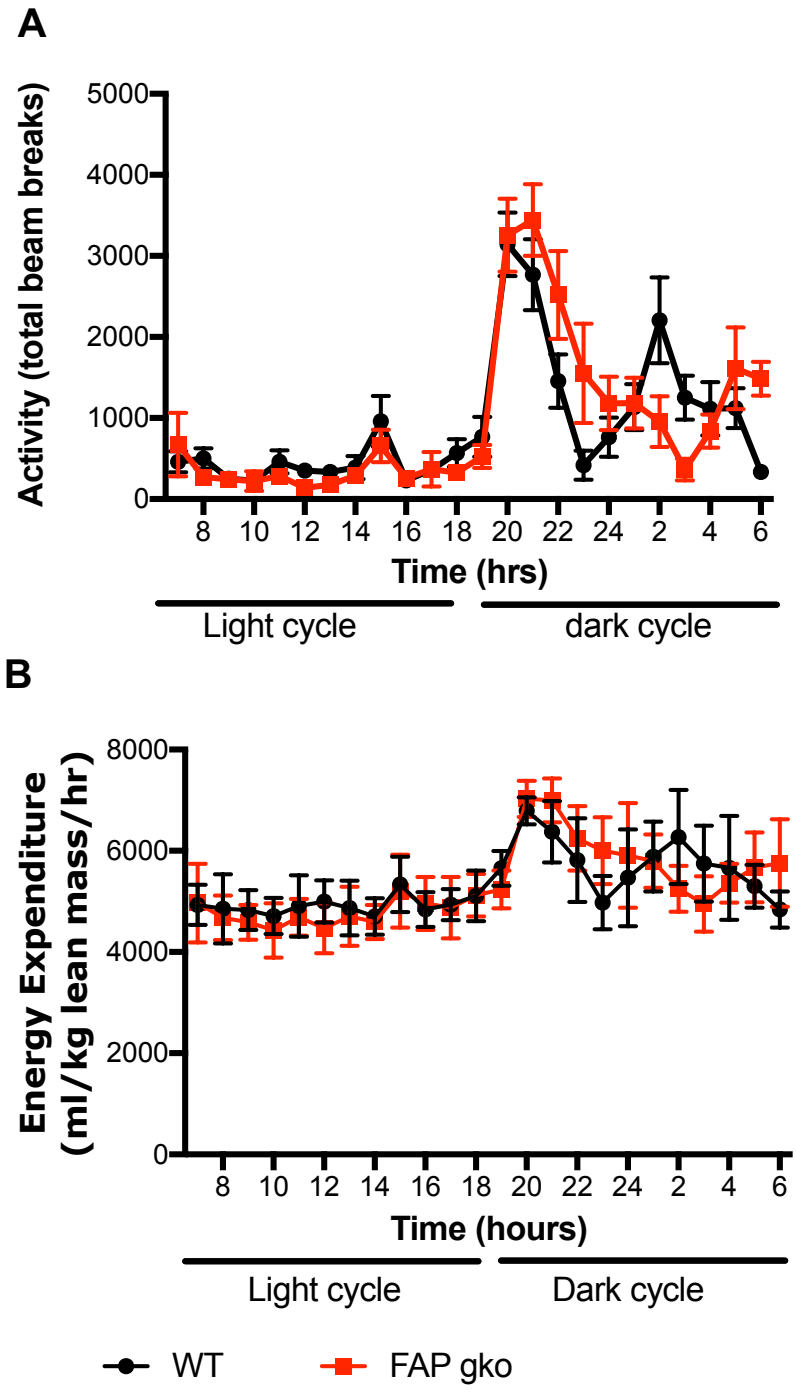
A
Activity (total beam breaks)
5000
4000
3000
2000
1000
0
8 10 12 14 16 18 20 22 24 2 4 6
Time (hrs)
Light cycle
dark cycle
B
Energy Expenditure (ml/kg lean mass/hr)
8000
6000
4000
2000
0
8 10 12 14 16 18 20 22 24 2 4 6
Time (hours)
Light cycle
Dark cycle
WT
FAP gko

Fig. S15

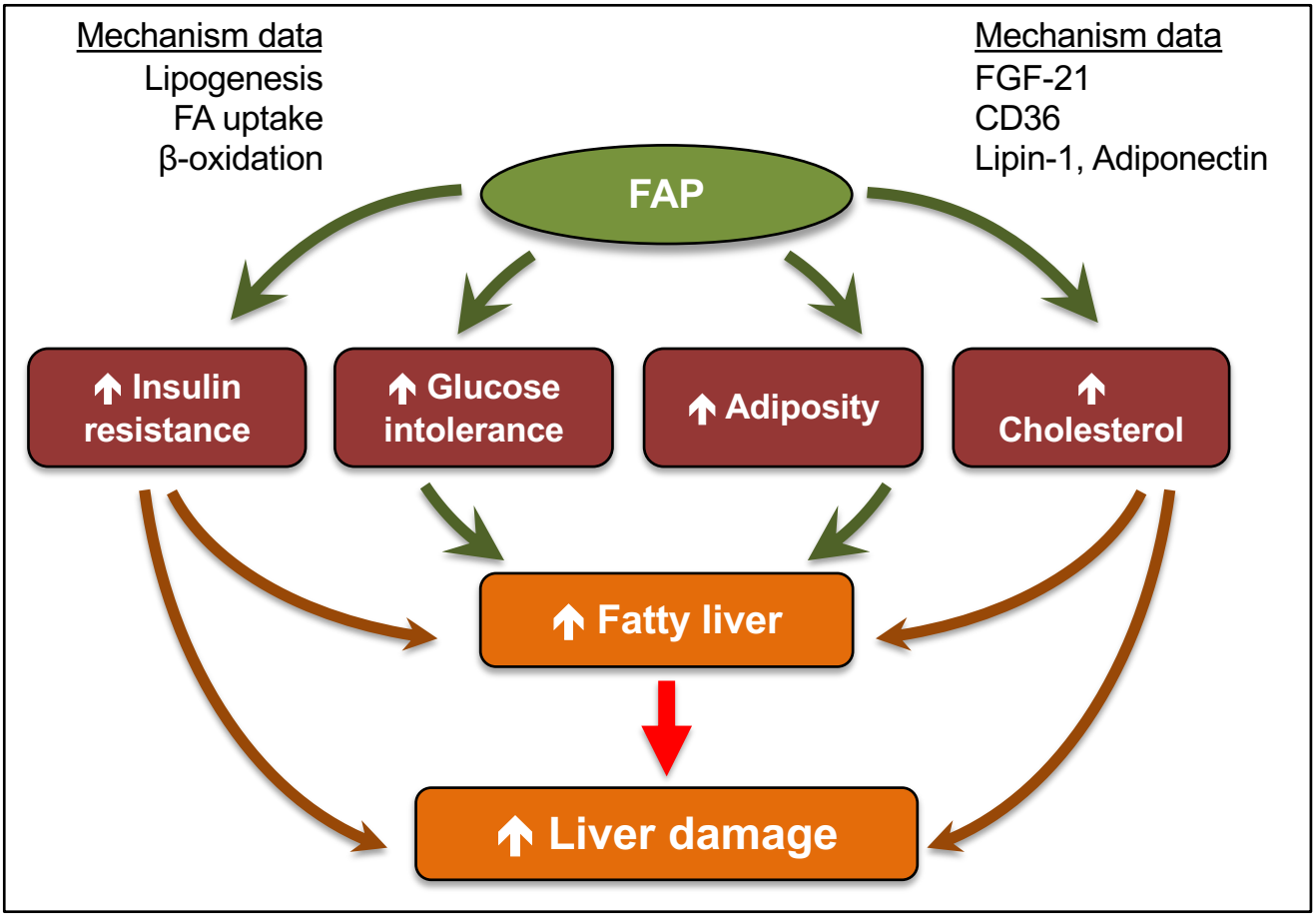
Mechanism data
Lipogenesis
FA uptake
β-oxidation
Mechanism data
FGF-21
CD36
Lipin-1, Adiponectin
FAP
↑ Insulin resistance
↑ Glucose intolerance
↑ Adiposity
↑ Cholesterol
↑ Fatty liver
↑ Liver damage

Fig. S16